THE JOURNAL OF BIOLOGICAL CHEMISTRY VOL. 285, NO. 21, pp. 16003–16011, May 21, 2010

Frequent Calcium Oscillations Lead to NFAT Activation in Human Immature Dendritic Cells*

Received for publication, September 16, 2009, and in revised form, March 25, 2010 Published, JBC Papers in Press, March 26, 2010, DOI 10.1074/jbc.M109.066704

Mirko Vukcevic[‡], Francesco Zorzato[‡§], Giulio Spagnoli[¶], and Susan Treves[‡§1]

From the [‡]Departments of Anaesthesia and Biomedicine and the [¶]Institute of Surgical Research, Basel University Hospital, Basel 4031, Switzerland and the [§]Department of Experimental and Diagnostic Medicine, General Pathology Section, University of Ferrara, Ferrara 44100, Italy

Spontaneous Ca^{2+} oscillations have been observed in a number of excitable and non-excitable cells, but in most cases their biological role remains elusive. In the present study we demonstrate that spontaneous Ca^{2+} oscillations occur in immature human monocyte-derived dendritic cells but not in dendritic cells stimulated to undergo maturation with lipopolysaccharide or other toll like-receptor agonists. We investigated the mechanism and role of spontaneous Ca^{2+} oscillations in immature dendritic cells and found that they are mediated by the inositol 1,4,5-trisphosphate receptor as they were blocked by pretreatment of cells with the inositol 1,4,5-trisphosphate receptor antagonist Xestospongin C and 2-aminoethoxydiphenylborate. A component of the Ca^{2+} signal is also due to influx from the extracellular environment and may be involved in maintaining the level of the intracellular Ca^{2+} stores. As to their biological role, our results indicate that they are intimately linked to the "immature" phenotype and are associated with the translocation of the transcription factor NFAT into the nucleus. In fact, once the Ca^{2+} oscillations are blocked with 2-aminoethoxydiphenylborate or by treating the cells with lipopolysaccharide, NFAT remains cytoplasmic. The results presented in this report provide novel insights into the physiology of monocyte-derived dendritic cells and into the mechanisms involved in maintaining the cells in the immature stage.

Dendritic cells (DCs)[2] are the most potent antigen presenting cells and are thought to be the initiators and modulators of the immune response (1). In general, DCs exist in two forms, immature DCs (iDC) and mature DCs. Immature DCs are extremely efficient at endocytosis; they reside in the peripheral tissues and continuously sample their environment for the presence of foreign antigens. After capturing antigens, they become activated and migrate to the lymphoid tissues and in the process lose the ability to take up new antigens, increase their surface expression of major histocompatibility complex II molecules and co-stimulatory molecules involved in antigen presentation to T cells, and reach their full maturation stage (1–3). Although generally correct, this picture is now proving to be too simple. For example, it was recently found that iDCs are also involved in induction and maintenance of T cell tolerance in peripheral tissues (4).

Immature DCs, produced by culturing monocytes for 5 days in medium containing granulocyte-macrophage stimulating factor and interleukin-4 (IL-4), are phenotypically, morphologically, and functionally identical with iDCs occurring *in vivo* (5). Their maturation is controlled by Toll-like receptors (TLRs), one of the best characterized classes of pattern recognition receptors of mammalian species. Most mammalian species express about 10–15 different TLRs that are encoded by a yet to be defined number of genes. Interestingly, distinct subsets of DCs express different TLRs, and their engagement results in DC maturation (6). In fact, monocyte-derived DCs can be induced to mature very efficiently by incubating them with nanogram to microgram (per ml) concentrations of lipopolysaccharide (LPS) through engagement of TLR4 receptors (7). In addition, other ligands such as the synthetic TLR7 ligand imidazoquinoline, a reagent already used as adjuvant in the treatment of viral infections and skin tumors (8–10), can also induce maturation of iDCs *in vitro*. The signaling pathways leading to DC maturation are complex and involve nuclear translocation of the transcription factor NF-κB as well as increases in the cytoplasmic Ca^{2+} concentration ($[Ca^{2+}]$) (11–15). Ca^{2+} is one of the most ubiquitous second messengers underlying cellular responses such as secretion, motility, proliferation, and death. Interestingly, Ca^{2+}-sensitive transcription factors including NFAT and NF-κB regulate the expression of Ca^{2+}-sensitive genes including IL-2, IL-3, IL-4, tumor necrosis factor-α, and interferon-γ (16, 17). Some cell types exhibit oscillatory changes of their cytosolic Ca^{2+}, and these have been correlated to a variety of cellular functions. For example, in T-cells, depending on their frequency, oscillations trigger Ca^{2+}-dependent activation of the transcription factors NFAT, NF-κB, and c-Jun N-terminal kinase (JNK) (18). In human bone marrow-derived mesenchymal stem cells, Ca^{2+} oscillations have been implicated in differentiation (19), in embryonic stem cell-derived primitive endodermal cells, oscillations have been implicated in the exo/endocytotic vesicle shuttle (20), and in human astrocytoma cells Ca^{2+} oscillations have been implicated in cell migration (21). Ca^{2+} signaling is also known to be involved in the regulation of immune cell function, and its

* This work was supported by Swiss National Science Foundation Grants SNF 3200B0-114597 and 3200B0-104060.

[1] To whom correspondence should be addressed: Depts. of Anesthesia and Biomedical Research, Basel University Hospital, Hebelstrasse 20, 4031 Basel, Switzerland. Tel.: 41-61-2652373; Fax: 41-61-2653702; E-mail: susan.treves@unibas.ch.

[2] The abbreviations used are: DC, dendritic cell; $[Ca^{2+}]_i$, intracellular calcium concentration; iDC, immature DC; LPS, lipopolysaccharide; NFAT, nuclear factor of activated T-cells; NF-κB, nuclear factor κ-light-chain enhancer of activated B cells; DAPI, 4′ 6-diamidino-2-phenylindole, dihydrochloride; 2-APB, 2-aminoethoxydiphenyl borate; IL-4, interleukin-4; TLR, Toll-like receptor; $InsP_3R$, inositol-1,4,5-trisphosphate receptor; TIRF, total internal reflection fluorescence; FITC, fluorescein isothiocyanate.

importance is emphasized by the fact that most immune cells including DCs express several classes of Ca^{2+} channels on their plasma membrane (22) as well as intracellular Ca^{2+} channels belonging to the $InsP_3R$ and ryanodine receptor family (23–28). In this context it is worth mentioning that the involvement of Ca^{2+} signaling events in DC maturation has been postulated for a number of years (14, 15), and we recently demonstrated that ryanodine receptor 1-mediated Ca^{2+} signals can act synergistically with signals generated via Toll-like receptors driving DC maturation (26, 27).

In the present report we show that spontaneous Ca^{2+} oscillations occur in iDCs. These oscillations occur only in iDCs and are lost during the maturation process, and their abrogation leads to the cytoplasmic localization of endogenous NFAT. The results of this study offer additional insights into some of the signaling processes controlling maturation of DCs.

MATERIALS AND METHODS

Generation of Dendritic Cells—iDCs were generated from human peripheral blood mononuclear cells as previously described (29). Briefly, monocytes were purified by positive sorting using anti-CD14-conjugated magnetic microbeads (Miltenyi Biotech, Bergisch Gladbach, Germany). The recovered cells (95–98% purity) were cultured for 5 days at $3–4 \times 10^5$/ml in differentiation medium containing RPMI with 10% fetal calf serum, glutamine, nonessential amino acids, and antibiotics (all from Invitrogen) supplemented with 50 ng/ml granulocyte-macrophage stimulating factor (Laboratory Pablo Cassarà, Buenos Aires, Argentina) and 1000 units/ml IL-4 (a gift from A. Lanzavecchia, Institute for Research in Biomedicine, Bellinzona, Switzerland). Maturation was induced by the addition of LPS 1 μg/ml (from *Salmonella abortus equi*, Sigma) to the culture medium. In some experiments DC maturation was induced by the addition of the synthetic TLR7 agonist, imidazoquinoline (3M-001) (final concentration 3 μM), that was kindly provided by 3M Pharmaceuticals (St. Paul, MN).

Single Cell Intracellular Ca^{2+} Measurements—Ca^{2+} measurements were performed on DCs loaded with fast Ca^{2+} indicator fluo-4 (Invitrogen; 5 μM final concentration). In some experiments cells were incubated with 100 μM 2-aminoethoxydiphenylborate (2-APB) (Calbiochem), 1 μM Xestospongin C (Calbiochem), or 2 μM thapsigargin with 0.5 mM EGTA during the loading procedure. After loading, cells were rinsed once, resuspended in Krebs-Ringer medium, and allowed to adhere to poly-L-lysine (1:60 dilution) (Sigma)-treated glass coverslips that were than mounted onto a 37 °C thermostatted chamber. On-line epifluorescence images were acquired every 100 ms for 50 s using a Nikon Eclipse TE2000-E fluorescent microscope equipped with an oil immersion CFI Plan Apochromat 60× TIRF objective (1.45 numerical aperture). Changes in fluorescence were detected by exciting at 488 nm and recording the emission at 510 nm via an electron multiplier C9100–13 Hamamatsu CCD camera which allows fast data acquisition (maximal temporal resolution 1 frame (110×110 pixels/8 ms). Where indicated, either 1 μg/ml LPS or 2 μM U73122 (Bio Mol) was added during the measurements. To investigate the dynamics of Ca^{2+}influx, we measured fluorescent changes in the TIRF mode; first we identified the focal plane at the coverglass/cell membrane contact with a surface reflective interference contrast filter, and this focal plane was maintained throughout the recordings by means of the perfect focus system that exploits an infrared laser beam and a quadrant diode for online control of the microscope focusing motor. Image analysis was performed with the MetaMorph (Molecular Devices) software package.

Endocytosis and Quantitative Gene Expression Analysis—Endocytosis was followed by incubating DCs in RPMI medium containing 0.5 mg/ml fluorescein isothiocyanate (FITC)-labeled dextran (Fluka Biochemicals, Buchs, Switzerland) for 30 min at 37 °C. Cells were washed twice in ice-cold phosphate-buffered saline fixed with 1% paraformaldehyde, and the number of FITC-positive cells was assessed by flow cytometry. In some experiments, before incubation with FITC-dextran, cells were treated for 45 min with 100 μM 2-APB or with LPS (1 μg/ml) or with the TLR-7 agonist 3M-001 (3 μM) for 18 h. Gene expression was quantified by real time PCR as previously described (26). Briefly, $1–2 \times 10^6$ iDCs were incubated for 18 h with 1 μM Xestospongin C, 100 μM 2-APB, 3 μM imidazoquinoline (3M-001), or 1 μg/ml LPS. Total RNA was extracted and treated with deoxyribonuclease I (Invitrogen) to eliminate contaminant genomic DNA. After reverse transcription using 500 ng of RNA and the Moloney murine leukemia virus reverse transcriptase (Invitrogen), cDNA was amplified by quantitative real-time PCR in the ABI PrismTM7700 using the TaqMan® technology. Commercially available exon-intron junction-designed primers for glyceraldehyde-3-phosphate dehydrogenase, CD83, CD80 CD86, interferon-α, and IL23A (Applied Biosystems, Forster City, CA) were used. Gene expression was normalized using self-glyceraldehyde-3-phosphate dehydrogenase as reference (26). The data from DCs isolated from five donors were pooled and are expressed as -fold increase in gene expression compared with untreated iDCs.

Immunofluorescence—Indirect immunofluorescence was performed on methanol:acetone (1:1)-fixed DCs using rabbit anti-NFATc1 (sc-13033) or rabbit anti- NF-κB p65 antibody (sc-109, Santa Cruz Biotechnology) followed by Alexa fluor 488-conjugated chicken anti-rabbit antibody (Invitrogen). Nuclei were visualized by 4′ 6-diamidino-2-phenylindole, dihydrochloride (DAPI; 100 μM) (Invitrogen) staining. Fluorescence was detected using a fluorescent Axiovert S100 TV inverted microscope (Carl Zeiss GmbH, Jena, Germany) equipped with an ×40 FLUAR objective and Zeiss filter sets (BP 475/40, FT 500, and BP 530/50; BP 546, FT 560, and 575–640) for detection of DAPI and FITC fluorescence, respectively.

Immunoblotting Analysis—The cytosolic fraction of 6×10^6 DCs was extracted as described by Healy *et al.* (30). Briefly, cells were washed once and resuspended in 50 μl of ice-cold buffer containing 20 mM HEPES, pH 7.5, 5 mM NaCl, and 2 mM EDTA to which 50 μl of 20 mM HEPES, pH 7.5, 4 mM NaCl, 2 mM EDTA, and 0.8% Nonidet P-40 were added. Cells were incubated on ice for 2 min, and the nuclear and membrane fractions were removed by centrifugation ($600 \times g$, 10 min, 4 °C). Laemmli loading buffer (10% glycerol, 1% β-mercaptoethanol, 2% SDS, 65 mM Tris-HCl, pH 6.8) was added to the supernatant (cytosolic fraction) which was boiled for 5 min and then loaded onto a 7.5% SDS-polyacrylamide gel. Proteins were transferred

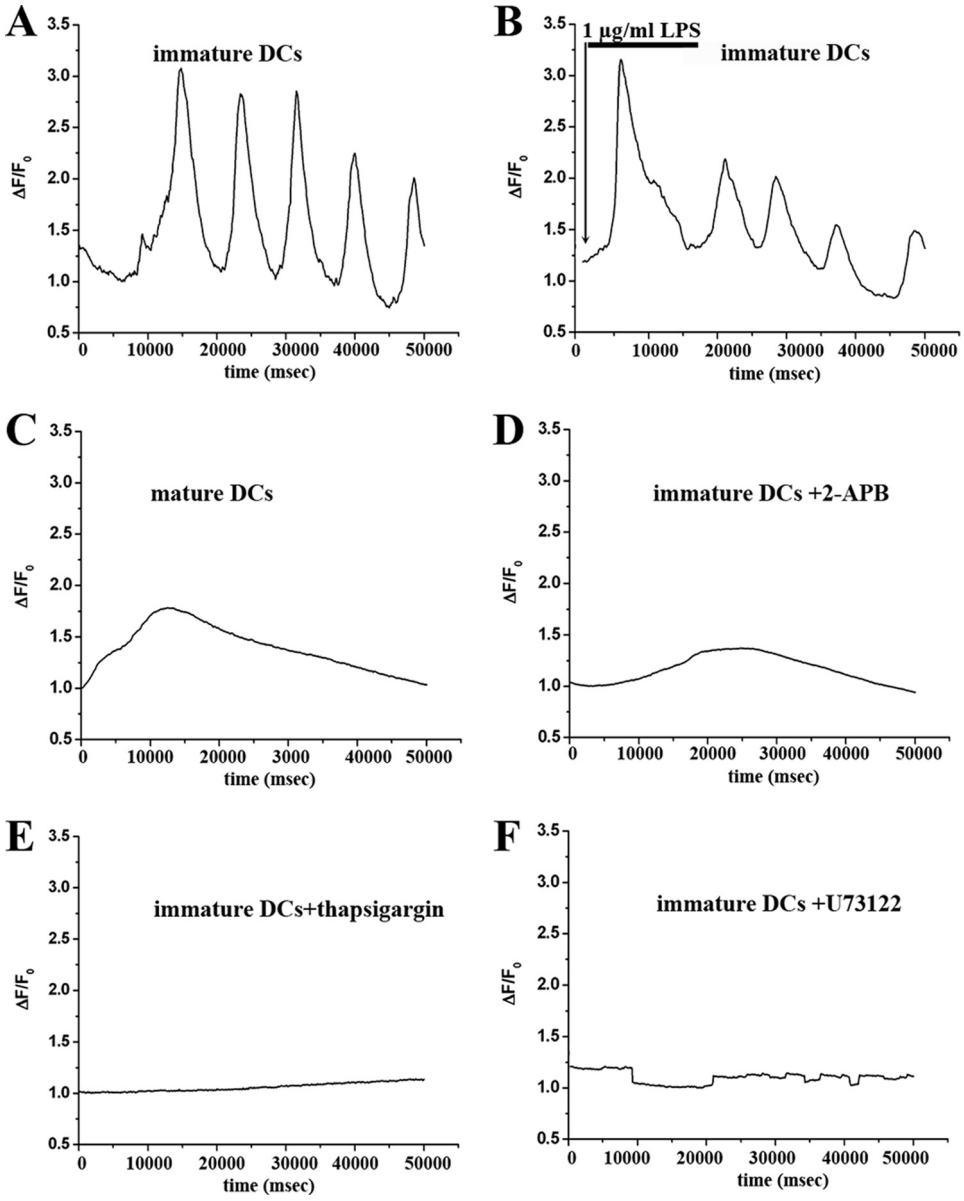

FIGURE 1. **Immature human dendritic cells show spontaneous Ca^{2+} oscillations.** Fluo-4-loaded dendritic cells were allowed to deposit on poly-L-lysine-treated coverslips, and the changes in fluo-4 fluorescence were monitored every 100 ms as described under "Materials and Methods." Shown is a representative trace of the oscillations observed in immature DCs (*A*), in iDCs to which 1 μg/ml LPS was added (*arrow*) (*B*), in dendritic cells treated with LPS (1 μg/ml) overnight (mature DCs) (*C*), in iDCs pretreated with 2-APB for 45 min (*D*), in iDCs pretreated with 2 μM thapsigargin and 0.5 mM EGTA (*E*), and in iDCs treated with the PLC-inhibitor U73122 (2 μM) (*F*). Traces are representative of experiments carried out on cells from five different donors. Results are expressed as F/F_o, where F is the fluorescent value at any given time, and F_o is the initial fluorescence level obtained at time 0.

TABLE 1

Characterization of spontaneous Ca^{2+} oscillations in DCs

Frequency is represented as a percentage of cells with 1, 2–4, and 4–8 peaks during 50 s. Statistical analysis was performed using the χ^2 test. $p < 0.0001$. All groups were significantly different compared to iDC $p < 0.002$.

	Total no. cells	1 peak/ 50 s	2–4 peaks/ 50 s	4–8 peaks/ 50 s
		%	%	%
iDC	83	8.30	51.70	40.00
iDC+ 100 μM La^{3+}	60	36.70	45	18.33
iDC+ 0.5 mM EGTA	66	28.80	53.80	17.40
iDC+ 100 μM 2-APB	116	100	0	0
iDC+ 1 μM Xesto C	56	48.21	41	10.71
LPS-matured DC	162	100	0	0
TLR7-matured DC	266	70.00	20.00	10.00

onto nitrocellulose, and the blots were probed with a rabbit anti-NFATc1 antibody (1:500; sc-13033, Santa Cruz Biotechnology) followed by peroxidase-conjugated protein G (1:250,000) and with mouse anti-β tubulin (Santa Cruz sc-5274) followed by peroxidase-conjugated anti-mouse IgG (1:200,000). The immunopositive bands were visualized by autoradiography using the Super Signal West Dura chemiluminescence kit from Thermo Scientific (for NFAT) and BM chemiluminescence kit from Roche Applied Science (for β-tubulin).

Statistical Analysis and Software Programs—Statistical analysis was performed using Student's *t* test for paired samples; means were considered statistically significant when the p value was <0.05. When more than two samples were compared, analysis was performed by the ANOVA test followed by the Bonferroni post hoc test. The PROC MIXED statistical analysis program (SAS 9.2) on log-transformed data were used for real-time PCR gene expression analysis from independent biological replicates. The Origin computer program (Microcal Software, Inc., Northampton, MA) was used to generate graphs and for statistical analysis. Statistical analysis of categorical data was performed using the χ^2 test for contingency tables with a 0.05 level of significance using R software (R development Core team 2008; R Foundation for Statistical Computing, Vienna, Austria; ISBN 3-900051-07-0) was used to perform χ^2 tests.

RESULTS

Immature DCs were loaded with the fast calcium indicator fluo-4 and were observed by conventional epifluorescence microscopy in the absence of added stimuli. Such cells display large rhythmic fluctuations of their cytoplasmic Ca^{2+} (Fig. 1*A*) with ~40% of the cells exhibiting oscillations with a frequency of one peak every 12.5 s (Table 1). Interestingly, the addition of LPS (Fig. 1*B*) or of the TLR-7 agonist (not shown) to iDCs did not affect the high frequency oscillations nor did it cause any immediate changes in the $[Ca^{2+}]_i$. On the other hand, when mature DCs (treated with 1 μg/ml LPS for 18 h) were observed under identical conditions, the high frequency oscillations were no longer present (Fig. 1*C*). In the latter case of the 162 individual cells that were monitored,

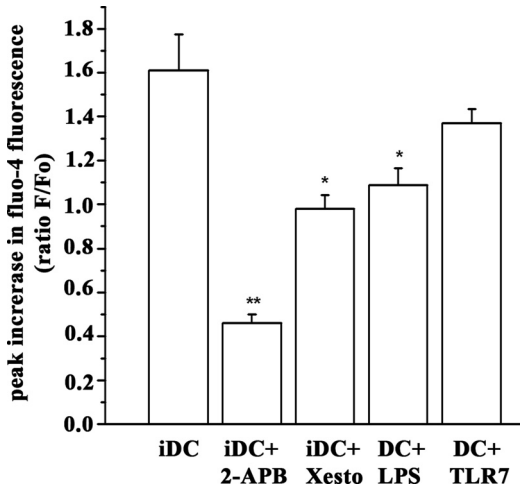

FIGURE 2. **Magnitude of spontaneous Ca^{2+} oscillations in DCs.** The histograms show the peak Ca^{2+} transient ($\Delta F/F_o$) in untreated iDCs or cells treated as indicated with 2-APB (100 μM), Xestospongin C (*Xesto*; 1 μM), and LPS (1 μg/ml 18 h). Experiments were performed on cells isolated from at least four different donors, and results are expressed as the mean (±S.E.) peak in fluo-4 fluorescence of 26–145 cells. Statistical analysis was performed using the ANOVA test followed by the Bonferroni post hoc test. *, $p < 0.015$; **, $p < 0.0005$.

100% responded with a single, small increase of the $[Ca^{2+}]_i$ within the 50-s measurement (Table 1). To determine the source of Ca^{2+} in the oscillations, iDCs were treated with (i) 100 μM 2-APB, a blocker of store-operated Ca^{2+} entry, and of $InsP_3$-mediated Ca^{2+} release, (ii) 2 μM thapsigargin, a SERCA (sarco(endo)plasmic reticulum calcium ATPase) inhibitor that leads to depletion of intracellular Ca^{2+} stores, and (iii) 2 μM U73122, an inhibitor of phospholipase C. The addition of these compounds completely abolished the spontaneous Ca^{2+} oscillations (Fig. 1, *D–F*). DCs were also incubated with other pharmacological agents as shown in Table 1; the addition of 100 μM La^{3+} or 0.5 mM EGTA significantly reduced the frequency of oscillations from 40% cells showing 4–8 peaks/50 s to about 18% cells showing 4–8 peaks/50 s, indicating that Ca^{2+} influx plays some role in the oscillatory events. The addition of 1 μM Xestospongin C (an inhibitor of $InsP_3$-mediated Ca^{2+} release) significantly diminished the frequency of the oscillations (Table 1) as well as the peak fluo-4 fluorescence in iDCs (Fig. 2). These results strongly suggest that the oscillations are mainly due to $InsP_3$-mediated release of Ca^{2+} from intracellular stores, with a component (probably involved in store refilling) due to influx from the extracellular environment. The phenotype of mature DCs, on the other hand, was quite different irrespective of whether the cells had been induced to mature via TLR-4 activation (by overnight incubation with 1 μg/ml LPS) or via activation of TLR-7 (by overnight incubation with 3 μM imidazoquinoline (3M-001)). In fact, LPS-matured DCs did not show the high frequency oscillations but rather small and slow (1 peak/50 s) spontaneous fluctuations of their $[Ca^{2+}]_i$. Interestingly, incubation with imidazoquinoline, which does not transmit a maturation signal as strong as that conveyed by LPS (see CD83 expression in Fig. 5*A*), resulted in DCs with an intermediate phenotype; that is, with only a small proportion of cells showing 2–8 oscillations/min whose magnitude is comparable with that exhibited by iDCs (Table 1 and Fig. 2). The slow peak Ca^{2+} increase observed in mature DCs was reduced by more than 50% by the addition of 100 μM 2-APB (Fig. 2), whereas the peak transient observed in the presence of Krebs-Ringer medium containing no additional Ca^{2+} and 0.5 mM EGTA was not different from that observed in the presence of extracellular Ca^{2+} (1.79 ± 0.31 and 2.10 ± 0.35 ΔF increase in Ca^{2+} and EGTA containing medium respectively). These results indicate that in mature DCs as well, the slow Ca^{2+} transient is mainly do to release from intracellular stores.

To directly determine whether Ca^{2+} influx accompanies the oscillations, we examined the DCs by TIRF microscopy, which allows one to monitor changes in fluorescence occurring at the plasma membrane or within microdomains close to the plasma membrane. As shown in Fig. 3 oscillations are accompanied by $[Ca^{2+}]_i$ influx in iDCs. Cells were allowed to attach onto the glass coverslips, and the areas of attachment were identified with the surface reflection interference contrast filter (Fig. 3, *panel B*). This focal plane was fixed using the perfect focus system, and changes in the $[Ca^{2+}]_i$, which in this case represent Ca^{2+} events occurring at or very close to the plasma membrane, were monitored (Fig. 3, *panel C*). The pseudocolor images in *panel C* represent the changes of fluo-4 fluorescence ΔF (F/F_o) at four time points, whereas *panel D* represents the kymographs of three selected cells (*arrows* in *panel C*) showing that these changes in $[Ca^{2+}]_i$occur at different time points in different cells during the 50 s of recording. The specificity of the signal is demonstrated by the fact that the increase in fluo-4 fluorescence only occurs when cells are bathed in Krebs-Ringer solution containing 2 mM Ca^{2+} but is absent when cells are bathed in Krebs-Ringer solution containing 100 μM La^{3+} (a nonspecific blocker of plasma membrane Ca^{2+} channels) or in LPS-matured DCs (Fig. 3, *panel E*).

These results support the finding that oscillations of the $[Ca^{2+}]_i$ are a specific feature of iDC that is lost upon differentiation but convey little information as to their biological role. We hypothesized that oscillations may be implicated in maintaining the immature phenotype by acting on transcription factors, in particular on the Ca^{2+}-sensitive transcription factor NFAT. To dissect the intracellular pathways directly downstream of the spontaneous Ca^{2+} oscillations, we followed the intracellular localization of endogenous NFAT in oscillating iDCs or in DCs in which oscillations had been inhibited by 2-APB and in mature DCs. The cytosolic fraction of DCs was obtained from untreated iDCs, iDCs treated for 15 and 45 min with 2-APB, LPS-matured DCs, and iDCs treated with cyclosporine, a drug that reduces the nuclear translocation of NFAT by inhibiting the Ca^{2+}-dependent phosphatase calcineurin. Fig. 4*A* shows a representative Western blot and Fig. 4*B* shows a *bar graph* of the intensities of the immunopositive bands of the cytosolic content of NFATc1. LPS-matured DCs, which lack the high frequency Ca^{2+} oscillations, show the highest level of cytoplasmic expression of NFAT. Similarly, its cytoplasmic level is high in cyclosporine-treated iDCs but is significantly reduced in the cytoplasm of untreated iDCs. Treatment of the latter cells with 2-APB induced the cytoplasmic localization of NFATc1. Fig. 4*C* shows the subcellular localization of NFATc1 by immunofluorescence; indeed, in iDCs a number of cells exhibit nuclear distribution of NFAT (*arrows*), whereas iDCs

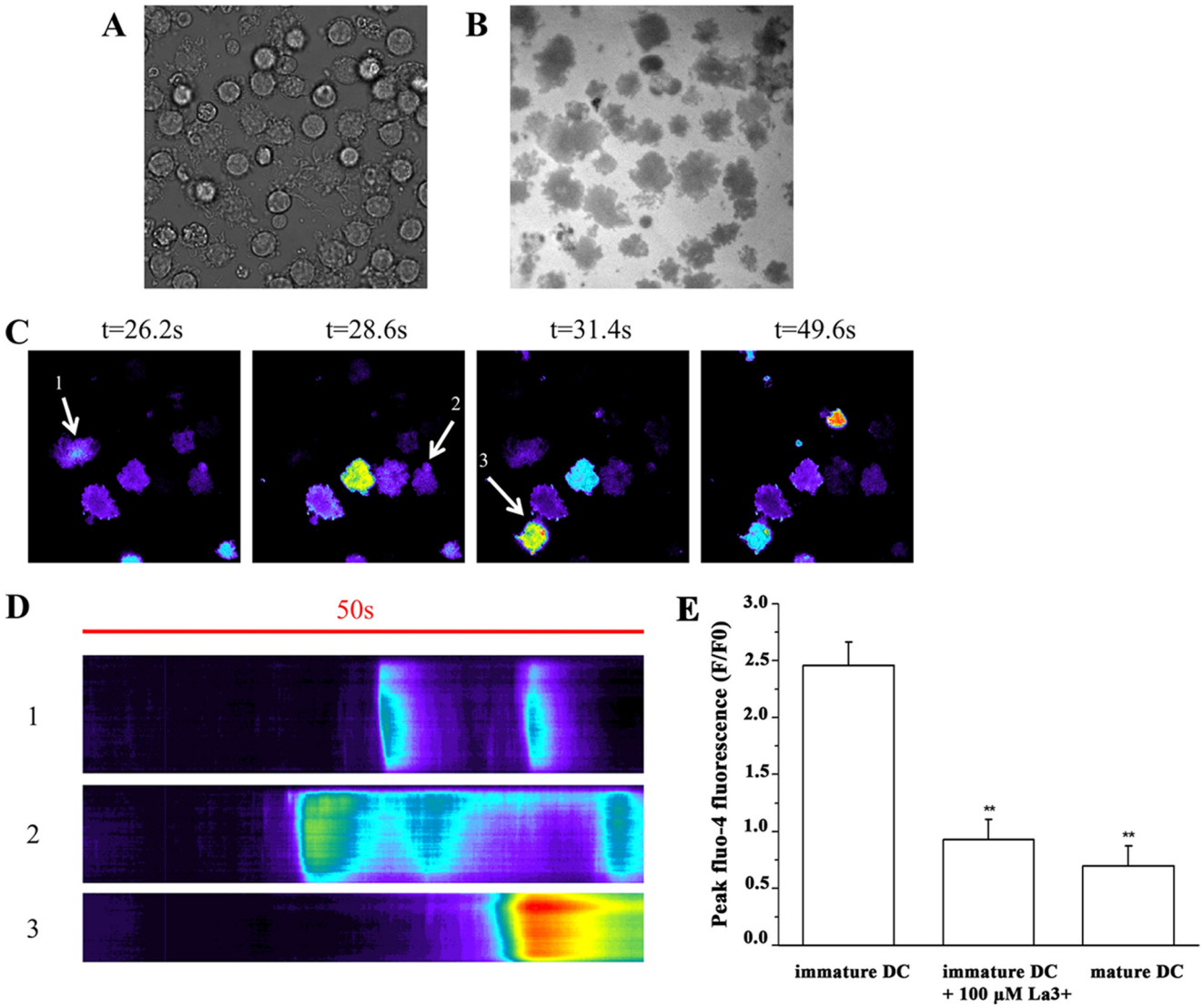

FIGURE 3. **Calcium influx in iDCs monitored by TIRF microscopy.** Fluo-4 loaded iDCs were resuspended in Krebs-Ringer medium containing 2 mM Ca^{2+} or 100 μM La^{3+} and allowed to attach to poly-L-lysine-coated glass coverslips. Once attached, cells were monitored by brightfield (*panel A*) with a surface reflection interference contrast filter to monitor glass coverslip/cell membrane attachment site (*panel B*) or by TIRF microscopy (*panel C*). Images in *panel C* show pseudocolored ratiometric (F/F_o) changes in membrane-associated $[Ca^{2+}]_i$ at four time points. *Panel D* shows the kymograph representation of the Ca^{2+} changes in 50 s in 3 selected cells from *panel C*. *Panel E* shows the mean (±S.E.) increase in fluo-4 fluorescence ratio (F/F_o) of iDCs bathed in 2 mM Ca^{2+} containing Krebs-Ringer medium ($n = 57$ cells), in iDCs bathed in Krebs-Ringer medium containing 100 μM La^{3+} ($n = 45$ cells), and in LPS-matured DCs ($n = 20$ cells). Experiments were performed on cells isolated from at least four different donors. **, statistical analysis was performed using the ANOVA test followed by the Bonferroni post hoc test $p < 0.0002$.

treated with cyclosporine or in mature DCs the fluorescence is distributed throughout the cytoplasm. These results indicate that most of the transcription factor NFAT is targeted to the nucleus in oscillating iDCs but that abrogation of Ca^{2+} oscillations with 2-APB results in the preservation of NFATc1 within the cytoplasm. To determine whether this was specifically related to the transcription factor NFAT or a general effect, we also followed the subcellular distribution of p65 (RelA), a component of the NF-κB transcription complex (NF-κB1+RelA+IkB) detectable in the cytoplasm of iDCs that translocates to the nucleus upon DC maturation (12, 13, 26). As shown in Fig. 4*D*, in LPS-matured DCs NF-κB is translocated to the nucleus, whereas in iDCs it shows a cytoplasmic distribution. Blocking high frequency oscillations with 2-APB does not result in the nuclear translocation of NF-κB. Thus, the simple abrogation of spontaneous Ca^{2+} oscillations is not sufficient to stimulate the cells to undergo maturation, whereas the oscillations appear to regulate nuclear targeting of NFAT and may be intimately linked to the immature phenotype. The latter hypothesis was tested by following the effect of abolishing the high frequency oscillations on the transcription of several genes characteristic of mature DCs. As shown in Fig. 5*A*, iDCs exhibit low transcription levels of CD80, CD86, CD83, interferon-α, and IL23A, genes that are characteristically transcribed in mature DCs (1, 26, 31). Inhibition of high frequency Ca^{2+} oscillations with Xestospongin C or 2-APB caused a significant (2–20-fold) increase in their levels of expression.

Finally we studied whether the high frequency oscillations are linked to endocytosis, an essential phenotypic characteristic of iDCs (2, 3), by comparing the capacity of iDCs, 2-APB-

treated iDCs, and mature DCs to endocytose FITC-labeled dextran. Fig. 5*B* shows that although 2-APB reduces the percentage of FITC-positive cells by 40%, thus significantly reducing the endocytic activity of iDCs, it does not result in a loss of endocytosis comparable with that seen in mature DCs (loss of ~80%). These results strongly suggest that abolishing the Ca^{2+} oscillations generates a signal(s) required for DC maturation.

DISCUSSION

Spontaneous Ca^{2+} oscillations, which are rhythmic changes in $[Ca^{2+}]_i$ in the absence of stimulation, have been reported in certain types of excitable and non-excitable cells such as mesenchymal stem cells, endodermal cells, human astrocytoma cells, astrocytes, pancreatic acinar cells, cardiac myocytes, oocytes, and fibroblasts (19–21, 32–35), although their intracellular mediators and biological role(s) and the functional consequence of their inhibition have in many cases not been elucidated. In the present study we show that spontaneous Ca^{2+} oscillations also occur in human DCs and that these Ca^{2+} events are an exclusive characteristic of cells in the immature stage. In fact, the addition of LPS as well as maturation triggered by other stimuli leads to the loss of the spontaneous high frequency Ca^{2+} transients. A similar finding concerning the loss of spontaneous Ca^{2+} oscillations induced by differentiation was reported in human mesenchymal stem cells upon differentiation into adipocytes (19) and in osteogenic cells upon differentiation into osteoblasts (36, 37). Interestingly, in stem cells Ca^{2+} oscillations occur during the G_1 to S transition, suggesting their involvement in cell cycle progression (38, 39). On the other hand, i*n vitro* monocyte-derived DCs do not actively proliferate but, rather, acquire the biochemical and immunological characteristics of naturally occurring iDCs (5) indicating that in these cells the oscillations are probably not involved in cell division.

In immature dendritic cells, intracellular Ca^{2+} stores and $InsP_3$ are intimately connected with the high frequency oscillations, as they were completely abolished by depleting stores with the Ca^{2+}-ATPase inhibitor thapsigargin (2 μM) in the presence of EGTA (0.5 mM). The lack of high frequency Ca^{2+} oscillations in mature LPS-treated DCs could not be explained by different levels of expression of functional $InsP_3R$ as mature DCs respond to ATP an $InsP_3$-mobilizing agonist (23) with a Ca^{2+} transient of comparable magnitude in the

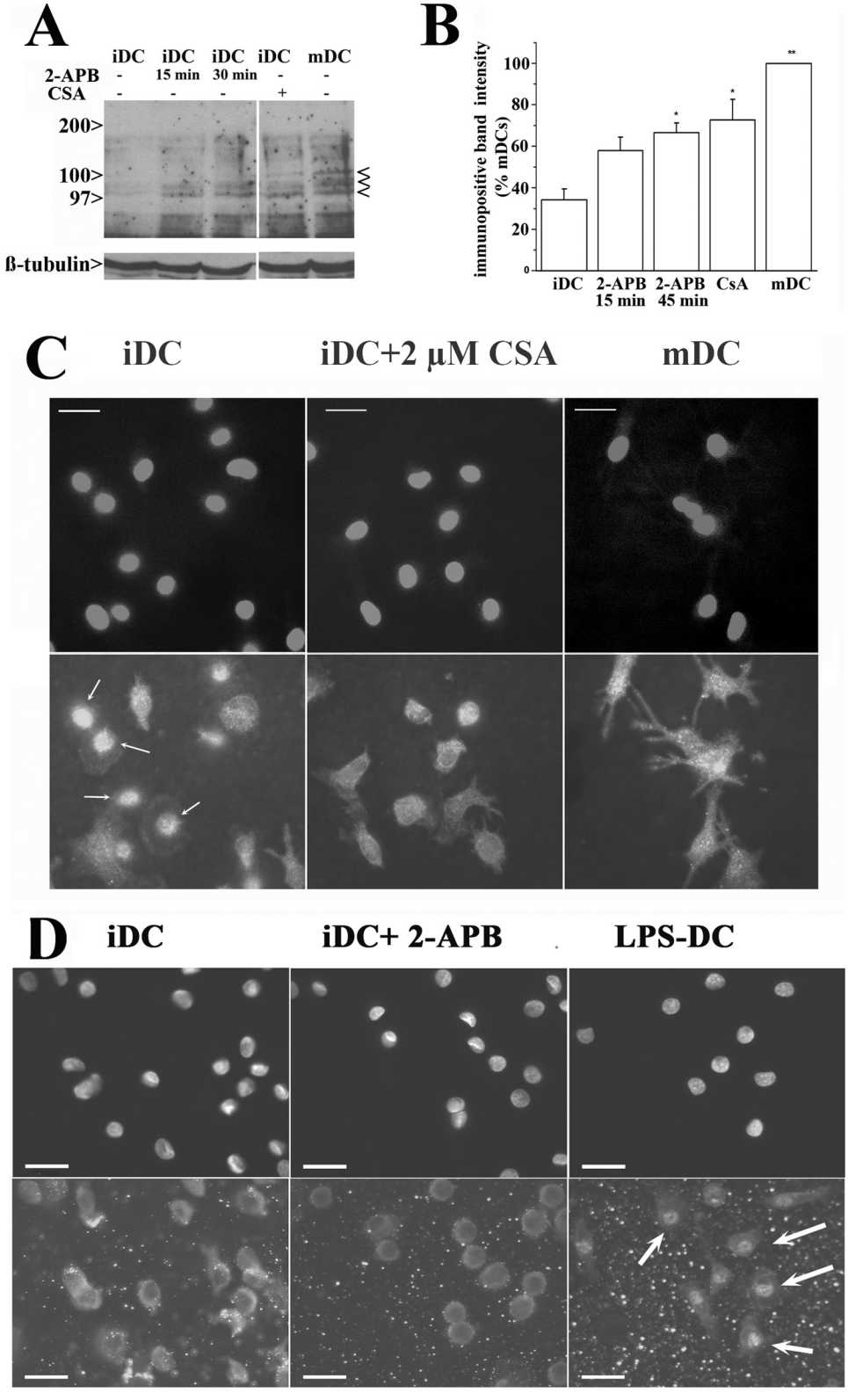

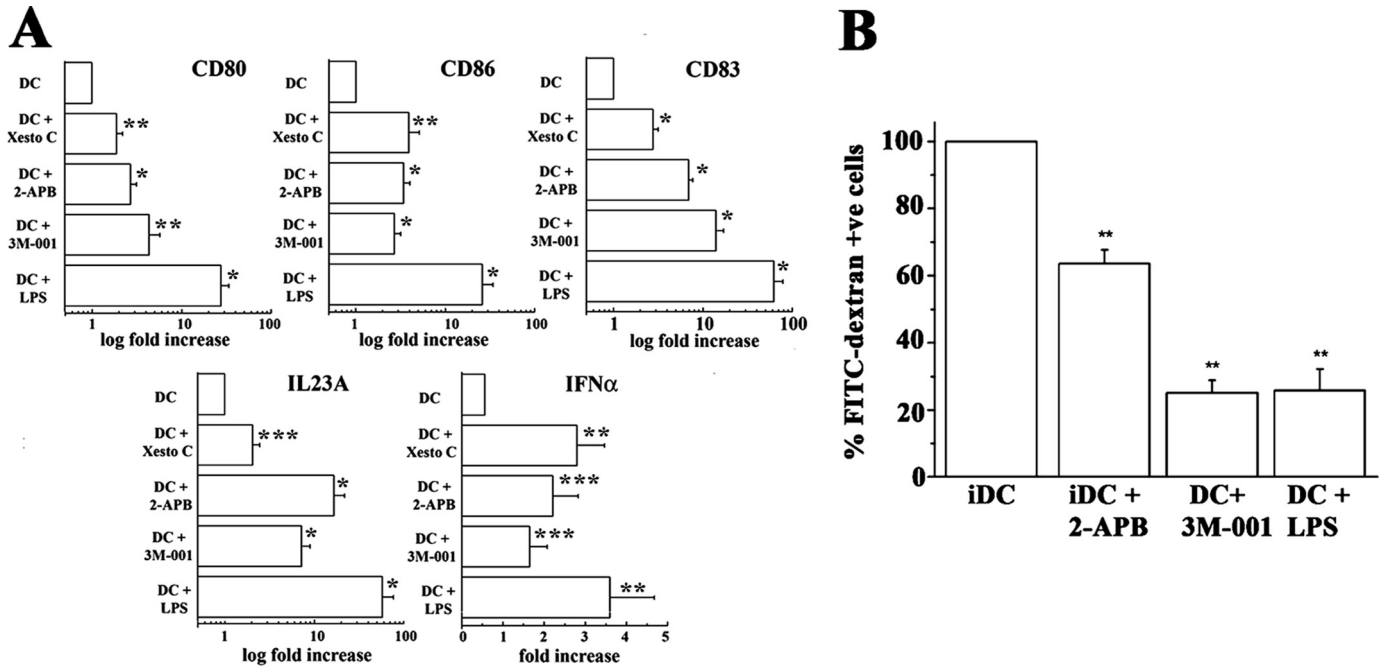

FIGURE 5. **Maturation markers of DCs after inhibition of oscillations.** *A*, real-time PCR analysis of genes involved in DC maturation in untreated cells or DCs treated for 18 h with Xestospongin C (1 μM), 2-APB (100 μM), TLR-7 agonist 3M-001 (3 μM), or LPS (1 μg/ml). Total RNA was extracted from 1–2 $\times$ 10^6 cells, and CD83, CD80, CD86, interferon-α, and IL23A gene expression was evaluated by quantitative real-time PCR. Gene expression results are expressed as mean ($\pm$S.E.)-fold increase as compared with values obtained in iDCs treated with medium. Pooled data are from experiments carried out on cells from five different donors except for CD83 (DC+3M-001), INFα (DC+2-APB, 3M-001, LPS), IL23A (DC+XestoC, DC+2-APB), where data from four donors were pooled, and CD83 (DC+2-APB), where data from three donors were pooled. Statistical analysis was performed using the PROC MIXED SAS 9.2 statistical analysis program. *, $p <$ 0.0001; **, $p < 0.00025$; ***, $p < 0.001$. *B*, endocytosis of FITC-labeled dextran is shown. Cells treated as described for *panel A* were plated in 12-well plate and incubated at 37 °C for 30 min with 0.5 mg/ml of FITC-labeled dextran. Negative controls were also incubated with FITC-labeled dextran but kept for 30 min at 4 °C. Cells were washed 2 times with ice-cold phosphate-buffered saline and fixed with 1% paraformaldehyde, and the % of FITC-positive (+*ve*) cells was assessed by flow cytometry. *Bar graphs* represent the mean ($\pm$S.E.) % of fluorescent cells; fluorescent value obtained for iDC was considered 100%. Results from 3–8 experiments from 3–8 different donors were pooled and averaged. Statistical analysis was performed using the ANOVA test followed by the Bonferroni post hoc test. *, $p < 0.018$; **, $p < 0.0003$.

mature and immature stage (results not shown). As to the intracellular mediator(s) of the Ca^{2+} oscillations, U73122, an inhibitor of phospholipase C (40), completely blocked Ca^{2+} transients, whereas both 2-APB, a rather unspecific inhibitor of the $InsP_3R$ also inhibiting Ca^{2+} entry (41, 42), and Xestospongin C, an inhibitor of $InsP_3R$-mediated Ca^{2+} release (43), significantly decreased the frequency and magnitude of these events. The differences in response to these compounds could be explained by the contribution of Ca^{2+} influx to the maintenance of the Ca^{2+} oscillations. To further address this question, we performed intracellular Ca^{2+} measurements in medium containing 2 mM Ca^{2+} or in the presence of 100 μM La^{3+} to block Ca^{2+} entry. Under these conditions Ca^{2+} fluctuations were still present, but there was a reduction in the percentage of cells showing high frequency (>4 transients/50 s) Ca^{2+} transients. This result together with the TIRF Ca^{2+} measurements support the hypothesis that Ca^{2+} influx is necessary to maintain the high frequency Ca^{2+} oscillations characteristic of immature dendritic cells through a refilling mechanism.

The most intriguing question arising from the observation that monocyte-derived dendritic cells in the immature stage show frequent Ca^{2+} oscillations concerns the biological role(s) of the oscillations. In macrophages, Ca^{2+} oscillations have been reported to accompany phagocytosis, suggesting a relationship between Ca^{2+} oscillations and uptake of foreign particles (44, 45). *In vivo*, immature DCs continuously sample their environment for foreign antigens, and indeed one of the main functions of iDCs is antigen capture by endocytosis. We originally

FIGURE 4. **Influence of Ca^{2+} oscillations on the intracellular localization of NFAT and NF-κB.** *A*, shown is a representative Western blot of the cytoplasmic fraction of iDCs treated as indicated and LPS (1 μg/ml)-matured DC (*mDCs*). In each lane the proteins present in the cytoplasmic extract of 6 $\times$ 10^6 cells was separated on 7.5% SDS-polyacrylamide gel and blotted onto nitrocellulose. The blot was cut into two; the *upper portion* (>60 kDa) was incubated with rabbit anti-NFATc1 followed by peroxidase-conjugated anti-rabbit IgG. The *lower portion* was used as a control for protein loading and developed with β-tubulin. Immunopositive bands were visualized by chemiluminescence; < indicates bands corresponding to NFAT. The experiment was repeated five times on DCs from different donors. *B*, the intensity of the immunopositive bands from five experiments was quantified by densitometry using Bio-Rad GelDoc 2000; the intensities were corrected for β-tubulin content. Values are expressed as % intensity of immunopositive bands of mature DCs. Statistical analysis was performed using the ANOVA test followed by the Bonferroni post hoc test. *, $p < 0.04$; **, $p < 0.00005$. *C*, shown is an immunofluorescence analysis of NFATc1 subcellular distribution in iDCs (untreated or treated with 2 μM cyclosporine (*CSA*)) and mature DC. Cells were fixed with an ice-cold solution of acetone: methanol (1:1) for 20 min at −20 °C. Cells were then incubated with rabbit anti-NFAT followed by Alexa fluor 488-labeled anti-rabbit IgG. Before mounting, DAPI staining was performed to visualize nuclei. The *scale bar* indicates 25 μm. *Arrows* indicate nuclear localization of NFAT in iDCs. *D*, NF-κB subcellular distribution in iDCs (untreated or incubated with 100 μM 2-APB for 45 min or with 1 μg/ml LPS for 60 min) is shown. Cells were fixed with an ice-cold solution of acetone:methanol (1:1) for 20 min at −20 °C. Cells were then incubated with rabbit anti- NF-κB p65 polyclonal antibody followed by Alexa fluor 488-labeled anti-rabbit IgG. Before mounting, DAPI staining was performed to visualize nuclei. The *scale bar* indicates 25 μm. *Arrows* indicate nuclear translocation of NF-κB in LPS-treated DCs.

hypothesized that the high frequency Ca^{2+} oscillations may be involved in activation of endocytosis, and blocking Ca^{2+} oscillations with 2-APB resulted in a significant but partial decrease of FITC-dextran endocytosis, suggesting that the high frequency oscillations may not be essential for endocytosis as reported in embryonic stem cell-derived primitive endodermal cells (20). Alternatively, the inhibitory effect of 2-APB may reflect the fact that endocytosis is a Ca^{2+}-dependent event requiring $InsP_3R$ activation and/or Ca^{2+} influx (46, 47). On the other hand, the involvement of Ca^{2+} signaling in maturation had been previously documented (26, 28), and it was shown that DC maturation is enhanced by activation of ryanodine receptor-mediated Ca^{2+} release. The results obtained by real time PCR strongly suggest that pharmacological interventions, which decrease the high frequency oscillations, activate signals that are necessary but not sufficient to induce full DC maturation.

We next turned our attention to Ca^{2+}-sensitive transcription factors as Ca^{2+} oscillations have been shown to promote the expression of specific genes in other cell systems (39, 48). We focused our attention on NFAT, a calcineurin-dependent transcription factor, as early work demonstrated that NFAT has the remarkable capacity to sense dynamic changes in the $[Ca^{2+}]_i$ and is especially tuned to detect high frequent Ca^{2+} oscillations occurring within cells (48, 49). In fact, high frequency oscillations have been shown to activate NFAT by keeping the transcription factor in the nucleus at high enough levels to bind to enhancer sites long enough to allow initiation of transcription. Because in our case only iDCs possess these high frequency Ca^{2+} fluctuations, NFAT should be active and translocated into the nucleus only in iDCs and not in LPS-matured DCs. Western blot analysis of endogenous NFAT indeed showed that the cytosolic fraction of iDCs contains considerable less immunopositive band compared with that present in mature DCs; furthermore, by shutting off the Ca^{2+} oscillations with 2-APB, NFAT is retained in the cytoplasm. As opposed to what was observed for NFAT, the transcription factor NF-κB is activated and translocated into the nucleus in LPS-matured DCs but not in iDCs nor in 2-APB-treated DCs. Thus, simply blocking the high frequency Ca^{2+} oscillations or blocking nuclear translocation of NFAT is not sufficient to induce either nuclear translocation of NF-κB or DC maturation.

Altogether these results indicate that the high frequency Ca^{2+} oscillations depend on the maturation stage of DCs, and we suggest that they act as "frequency encoding" (as opposed to amplitude encoding) signals, whereby through the activation of NFAT, DCs maintain their immature phenotype. Our data do not support recent results showing that LPS induces a transient increase in $[Ca^{2+}]_i$ in DCs (50–52). We directly tested whether the addition of LPS (1 μg/ml) to iDCs causes an increase in the cytoplasmic $[Ca^{2+}]_i$ but failed to obtain any response. Similarly, no changes in the $[Ca^{2+}]_i$ on plasma membrane microdomains after the addition of LPS were observed by TIRF microscopy (data not shown). The differences between our results and those presented in Refs. 50–52 are most likely due to the different experimental models that were used; that is, human monocyte-derived DCs in this study *versus* mouse bone marrow-derived DCs. In fact, as opposed to mouse DCs, immature human DCs express very low levels of CD14, and thus, the CD14-dependent Ca^{2+} signaling pathways may be absent in our system. Our possibility of using the TIRF microscope has enabled us to directly monitor membrane-associated events, and our results together with those of Matzner *et al.* (51) argue against a major role of Ca^{2+} influx in LPS-mediated Ca^{2+} signaling.

In conclusion, we report that human monocyte-derived iDCs exhibit spontaneous $[Ca^{2+}]_i$ oscillations that are linked to $InsP_3R$ activation and to, a lesser extent, to Ca^{2+} influx. These high frequency events are lost during maturation and appear to be an endogenous characteristic of the immature phenotype, possibly activating nuclear translocation of NFAT and, thus, enhancing the transcription of genes involved in maintaining the cells immature. The results of the present investigation are important because they point out novel aspects of intracellular signaling in human DC and may open new areas of research that could be developed in the future to help patients requiring modulation of their immune response.

Acknowledgments—We thank Dr. Andrija Tomovic for help with the statistical analysis. We also acknowledge the support of the Departments of Anesthesia and Surgery of Basel University Hospital.

REFERENCES

1. Banchereau, J., and Steinman, R. M. (1998) *Nature* **392,** 245–252
2. Trombetta, E. S., and Mellman, I. (2005) *Annu. Rev. Immunol.* **23,** 975–1028
3. Lanzavecchia, A. (1996) *Curr. Opin. Immunol.* **8,** 348–354
4. Mahnke, K., Schmitt, E., Bonifaz, L., Enk, A. H., and Jonuleit, H. (2002) *Immunol. Cell Biol.* **80,** 477–483
5. Sallusto, F., and Lanzavecchia, A. (1994) *J. Exp. Med.* **179,** 1109–1118
6. Iwasaki, A., and Medzhitov, R. (2004) *Nat. Immunol.* **5,** 987–995
7. Langenkamp, A., Messi, M., Lanzavecchia, A., and Sallusto, F. (2000) *Nat. Immunol.* **1,** 311–316
8. Hengge, U. R., and Ruzicka, T. (2004) *Dermatol. Surg.* **30,** 1101–1112
9. Urosevic, M., and Dummer, R. (2004) *Am. J. Clin. Dermatol.* **5,** 453–458
10. Bracci, L., Schumacher, R., Provenzano, M., Adamina, M., Rosenthal, R., Groeper, C., Zajac, P., Iezzi, G., Proietti, E., Belardelli, F., and Spagnoli, G. C. (2008) *J. Immunother.* **31,** 466–474
11. Bagley, K. C., Abdelwahab, S. F., Tuskan, R. G., and Lewis, G. K. (2004) *Clin. Diagn. Lab. Immunol.* **11,** 77–82
12. Ghosh, S., May, M. J., and Kopp, E. B. (1998) *Annu. Rev. Immunol.* **16,** 225–260
13. Lee, J. I., Ganster, R. W., Geller, D. A., Burckart, G. J., Thomson, A. W., and Lu, L. (1999) *Transplantation* **68,** 1255–1263
14. Koski, G. K., Schwartz, G. N., Weng, D. E., Czerniecki, B. J., Carter, C., Gress, R. E., and Cohen, P. A. (1999) *J. Immunol.* **163,** 82–92
15. Czerniecki, B. J., Carter, C., Rivoltini, L., Koski, G. K., Kim, H. I., Weng, D. E., Roros, J. G., Hijazi, Y. M., Xu, S., Rosenberg, S. A., and Cohen, P. A. (1997) *J. Immunol.* **159,** 3823–3837
16. Rao, A. (1994) *Immunol. Today* **15,** 274–281
17. Baeuerle, P. A., and Henkel, T. (1994) *Annu. Rev. Immunol.* **12,** 141–179
18. Lewis, R. S. (2003) *Biochem. Soc. Trans.* **31,** 925–929
19. Kawano, S., Otsu, K., Kuruma, A., Shoji, S., Yanagida, E., Muto, Y., Yoshikawa, F., Hirayama, Y., Mikoshiba, K., and Furuichi, T. (2006) *Cell Calcium* **39,** 313–324
20. Sauer, H., Hofmann, C., Wartenberg, M., Wobus, A. M., and Hescheler, J. (1998) *Exp. Cell Res.* **238,** 13–22
21. Rondé, P., Giannone, G., Gerasymova, I., Stoeckel, H., Takeda, K., and Haiech, J. (2000) *Biochim. Biophys. Acta* **1498,** 273–280
22. Hsu, Sf., O'Connell, P. J., Klyachko, V. A., Badminton, M. N., Thomson, A. W., Jackson, M. B., Clapham, D. E., and Ahern, G. P. (2001) *J. Immunol.* **166,** 6126–6133

23. Schnurr, M., Toy, T., Stoitzner, P., Cameron, P., Shin, A., Beecroft, T., Davis, I. D., Cebon, J., and Maraskovsky, E. (2003) *Blood* **102,** 613–620
24. Goth, S. R., Chu, R. A., Gregg, J. P., Cherednichenko, G., and Pessah, I. N. (2006) *Environ. Health Perspect.* **114,** 1083–1091
25. O'Connell, P. J., Klyachko, V. A., and Ahern, G. P. (2002) *FEBS Lett.* **512,** 67–70
26. Bracci, L., Vukcevic, M., Spagnoli, G., Ducreux, S., Zorzato, F., and Treves, S. (2007) *J. Cell Sci.* **120,** 2232–2240
27. Vukcevic, M., Spagnoli, G. C., Iezzi, G., Zorzato, F., and Treves, S. (2008) *J. Biol. Chem.* **283,** 34913–34922
28. Uemura, Y., Liu, T. Y., Narita, Y., Suzuki, M., Ohshima, S., Mizukami, S., Ichihara, Y., Kikuchi, H., and Matsushita, S. (2007) *Biochem. Biophys. Res. Commun.* **362,** 510–515
29. Schnurr, M., Toy, T., Shin, A., Hartmann, G., Rothenfusser, S., Soellner, J., Davis, I. D., Cebon, J., and Maraskovsky, E. (2004) *Blood* **103,** 1391–1397
30. Healy, J. I., Dolmetsch, R. E., Timmerman, L. A., Cyster, J. G., Thomas, M. L., Crabtree, G. R., Lewis, R. S., and Goodnow, C. C. (1997) *Immunity.* **6,** 419–428
31. Lutz, M. B., and Schuler, G. (2002) *Trends Immunol.* **23,** 445–449
32. Parri, H. R., Gould, T. M., and Crunelli, V. (2001) *Nat. Neurosci.* **4,** 803–812
33. Wang, T. F., Zhou, C., Tang, A. H., Wang, S. Q., and Chai, Z. (2006) *Acta Pharmacol. Sin.* **27,** 861–868
34. Fewtrell, C. (1993) *Annu. Rev. Physiol.* **55,** 427–454
35. Osipchuk, Y. V., Wakui, M., Yule, D. I., Gallacher, D. V., and Petersen, O. H. (1990) *EMBO J.* **9,** 697–704
36. Sun, S., Liu, Y., Lipsky, S., and Cho, M. (2007) *FASEB J.* **21,** 1472–1480
37. Kim, T. J., Seong, J., Ouyang, M., Sun, J., Lu, S., Hong, J. P., Wang, N., and Wang, Y. (2009) *J. Cell Physiol.* **218,** 285–293
38. Kapur, N., Mignery, G. A., and Banach, K. (2007) *Am. J. Physiol. Cell Physiol.* **292,** C1510–1518
39. Resende, R. R., Adhikari, A., da Costa, J. L., Lorençon, E., Ladeira, M. S., Guatimosim, S., Kihara, A. H., and Ladeira, L. O. (2010) *Biochim. Biophys. Acta* **1803,** 246–260
40. Smith, R. J., Sam, L. M., Justen, J. M., Bundy, G. L., Bala, G. A., and Bleasdale, J. E. (1990) *J. Pharmacol. Exp. Ther.* **253,** 688–697
41. Harks, E. G., Camiña, J. P., Peters, P. H., Ypey, D. L., Scheenen, W. J., van Zoelen, E. J., and Theuvenet, A. P. (2003) *FASEB J.* **17,** 941–943
42. Peppiatt, C. M., Collins, T. J., Mackenzie, L., Conway, S. J., Holmes, A. B., Bootman, M. D., Berridge, M. J., Seo, J. T., and Roderick, H. L. (2003) *Cell Calcium* **34,** 97–108
43. Gafni, J., Munsch, J. A., Lam, T. H., Catlin, M. C., Costa, L. G., Molinski, T. F., and Pessah, I. N. (1997) *Neuron* **19,** 723–733
44. Kruskal, B. A., and Maxfield, F. R. (1987) *J. Cell Biol.* **105,** 2685–2693
45. Myers, J. T., and Swanson, J. A. (2002) *J. Leukoc. Biol.* **72,** 677–684
46. Falcone, S., Cocucci, E., Podini, P., Kirchhausen, T., Clementi, E., and Meldolesi, J. (2006) *J. Cell Sci.* **119,** 4758–4769
47. Balaji, J., Armbruster, M., and Ryan, T. A. (2008) *J. Neurosci.* **28,** 6742–6749
48. Dolmetsch, R. E., Xu, K., and Lewis, R. S. (1998) *Nature* **392,** 933–936
49. Dolmetsch, R. E., Lewis, R. S., Goodnow, C. C., and Healy, J. I. (1997) *Nature* **386,** 855–858
50. Zanoni, I., Ostuni, R., Capuano, G., Collini, M., Caccia, M., Ronchi, A. E., Rocchetti, M., Mingozzi, F., Foti, M., Chirico, G., Costa, B., Zaza, A., Ricciardi-Castagnoli, P., and Granucci, F. (2009) *Nature* **460,** 264–268
51. Matzner, N., Zemtsova, I. M., Nguyen, T. X., Duszenko, M., Shumilina, E., and Lang, F. (2008) *J. Immunol.* **181,** 6803–6809
52. Aki, D., Minoda, Y., Yoshida, H., Watanabe, S., Yoshida, R., Takaesu, G., Chinen, T., Inaba, T., Hikida, M., Kurosaki, T., Saeki, K., and Yoshimura, A. (2008) *Genes Cells* **13,** 199–208